International Journal for Multidisciplinary Research (IJFMR)
E-ISSN: 2582-2160 ● Website: www.ijfmr.com ● Email: editor@ijfmr.com

Comparison of Leakage Property with Varying Lanthanum Doping in $(BiFeO_3)_{0.5}$-$(BaTiO_3)_{0.5}$

[1]Femina Brahma, S. Bhattacharjee[2], Santanu Sen[3], R.L. Hota[4], B. N. Parida[5]

[1]Department of Physics, Science College Kokrajhar, Kokrajhar-783370, Assam.
[2]Department of Physics, Kokrajhar Government College, Kokrajhar-783370, Assam.
[3,4,5]Department of Physics, Central Institute of Technology Kokrajhar, (Deemed to be University, MoE, Govt of India) BTR, Assam-783370.

Abstract:
The new La doped $BiFeO_3$-$BaTiO_3$perovskite oriented material is synthesized through solid state reaction route technique at an optimized temperature 1100^0C. The structural investigation through XRD technique suggesting the phase of the materials are orthorhombic and tetragonal. The dielectric investigation through the shifting of tangent of loss and dielectric coefficient with frequency over a specific range of temperature gives indication of overall good dielectric feature of the material. Besides NTCR feature of the material is identifies through impedance spectroscopy. The leakage feature investigated through I-V characteristic technique suggesting good insulating property of the material for device fabrication and the effect of the property with increasing doping.

Keywords: Perovskite; Dielectric; leakage; semiconducting

1. Introduction:

Now-a-days material scientists are more interested on perovskite materials for their fascinating characteristics. Perovskites are materials having the structure of ABO_3 which are smart materials. $BaTiO_3$ is the inorganic perovskite material which draws many attentions from material scientists for its excellent behaviors. Less dielectric loss and improved permittivity capacity, reduce the leakage current in perovskites. Incorporations had been taken in the B-site and A-site respectively by cations of $BaTiO_3$ materials. In earlier works it has been detected that doping or the replacement of Zr^{4+} for Ti^{4+} in BaTiO3 optimizes the leaky transportation assets and the dielectric trademarks.

To develop a multiferroic material perovskites are incorporated with several materials with magnetic ions in the recent past works either fully or partially. As the demand of time, to build a multifunctional device these kinds of materials having more than one characteristic draws many attentions. Among the materials of multiferroics, perhaps the most appreciated kind is the $BiFeO_3$ (BFO), which shows ferroelectric behavior with curie temperature~830^0C and anti-ferromagnetic with Neel temperature~370^0C as per the literature survey. The $6s^2$ "lone pair" of the Bi^{3+} ions and the 3d electrons of the Fe^{3+} ions are liable for the ferroelectric and anti-ferromagnetic occurrences in the BFO. as per the recent works. Leakage of lead from damaged perovskite solar modules during rainfall poses a serious threat to the environment and human

health. Strategies to replace lead have seen little success to date, while the encapsulation approaches tend to compromise the low-cost advantage of perovskites. [22]

Alloys with a high constant of dielectric and low losses of dielectric serve as essentials for technologies as they make it feasible to develop components. This has been realized through the inclusion of Lanthanum Ferrite (LaFeO3) Perovskite, also known as Orthoferrites, to BaTiO3. Since orthoferrites feature outstanding magnetic attributes and minimal loss, the participation was decided upon for this cause [8, 9]. Sorting of spin moments constitutes one of the many additional tangible advantages of orthoferrites. In contemplating this, further concurrently added Fe^{+3} and La^{+3} to $BaTiO_3$, yielding $(Bi_{0.75}La_{0.25}\ FeO_3)_{0.5}$ $(BaTiO_3)_{0.5}$ and $(Bi_{0.25}La_{0.75}\ FeO_3)_{0.5}$ $(BaTiO_3)_{0.5}$, and we inquired about its structural, dielectric, and leakage attributes.

2. Sample Preparation by the Solid Solution Synthesis Method:

The sample preparation task was approached via the solid oxide, adopted to create the polymorphic sample 1 which is $(Bi_{0.75}\ La_{0.25}\ FeO_3)_{0.5}$-$(BaTiO_3)_{0.5}$ and sample 2 which is $(Bi_{0.25}\ La_{0.75}\ FeO_3)_{0.5}$-$(BaTiO_3)_{0.5}$ adopting the appropriate proportions of the unprocessed components La_2O_3, $BaCO_3$, TiO_3, Bi_2O_3, and Fe_2O_3. The exorbitant amount-pure elements (>99%), picked from the manufactures of loba chemicals.

The above mentioned ingredients are first dry grinded for about 1 hour and then wet grinded in methanol for another 1 hour. The prepared sample was heated in high temperature furnace and the sample was formed at 1100^0C. The X-ray Diffraction analysis gives the assurance for the formation of the required compound, the solid solution of the material was palletized in the form of disc with the thickness of nearly 3 mm and diameter of 10mm, with polyvinyl Chloride and sintered at around 1150^0C for another 6 hours. The dielectric properties and I-V characteristics of the material is performed in the LCR meter for the frequency from 100Hz to 5 MHz in the temperature range of room temperature to 500^0C.

3. Results and Discussions:

3.1 Structural study:

The XRD pattern as shown in the Fig.1indicates that there are number of sharp peaks at defined at different Bragg's angles similar to raw material which confirms the formation of single phase new compound. The produced sample fits snugly into the orthorhombic structure after analysis in the "POWD" software. The projected unit cell encompasses the following probable values: for sample1, a = 7.11; b = 12.68; c=13.85 and V = 1249.56**(Å)³** and for sample 2 a=16.35; c=6.47; v=1733.61**(Å)³**, Utilising the Debye-Scherer formula, the cell/crystallite dimension of the samples were determined to be 23 nm and 66 nm respectively by the Debye Scherrer formula

$$\mathbf{D_{hkl} = k\lambda/\beta cos\theta_{hkl}}$$

where k = constant = 0.89, λ = 1.54050 A^0 and = full width at half maximum.

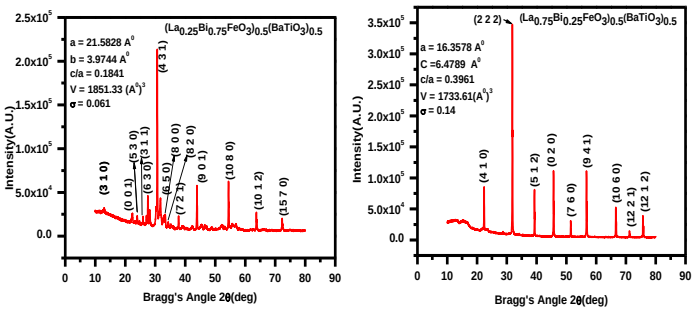

Fig.1 Shows the XRD pattern of the studied for sample1 and sample 2..

Tolerance factor is calculated using formula

$$t' = \frac{(r_A + r_O)}{\sqrt{2}(r_B + r_O)}$$

where r_A, r_B, and r_O are the cations' ionic radiuses, respectively, for the A, B, and oxygen anions (in Å unit), and it is found to be <1 which confirms that all structures are distorted from the ideal cubic symmetry.

3.2 Frequency dependent dielectric properties:

Fig.2 shows the dielectric property with frequency. The material's dielectric capability diminishes as frequency climbs and peaks in low frequency. High capacitance levels arise from polarisation at the junction, and low levels emerge as frequency-dependent improper alignment or phase mismatch of the dipoles occurs relative to local relative to the local pinning field direction.

As shown in the Fig.3 the dielectric loss or tan delta with frequency, it is predicted that at low frequency there is a relaxation peak with temperature and at high frequency the loss is low for every temperature variation. At lower frequency as the charge carriers require high energy to cross barrier of grain boundary results in high resistance and due to it the high loss but as the frequency raised the low resistance offered by grains gives the low value of loss. The relaxation peak represents the thermal activity in the material.

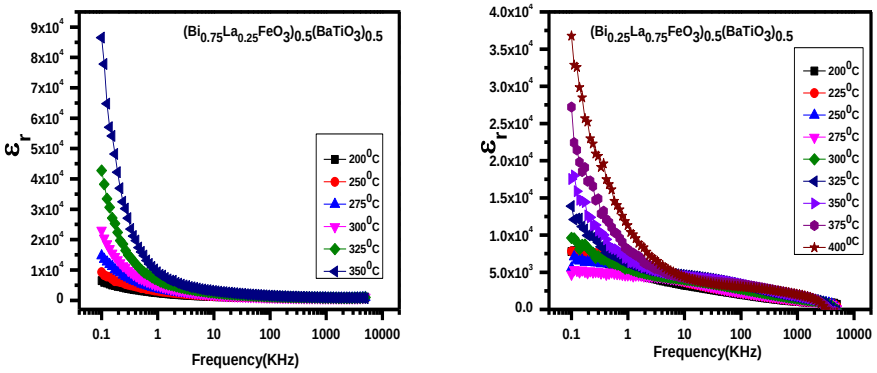

Fig.2 shows variation of dielectric and frequency

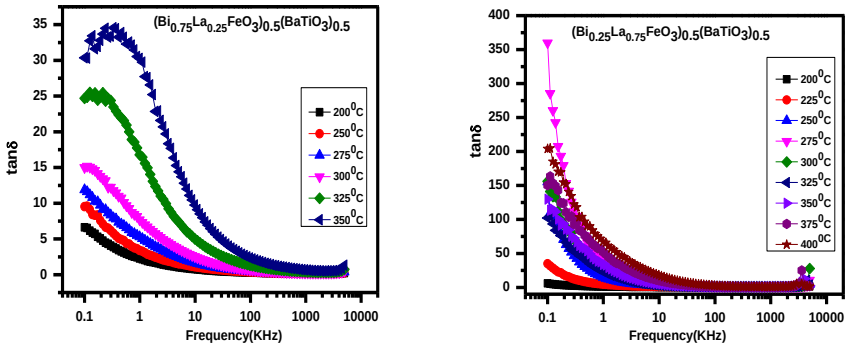

Fig.3 shows tangent loss variation with frequency

3.3 Complex impedance studies:

To analyse the electrical properties, impedance analysis is the most important tool. This analysis has given us the understanding of the contributions from the material's electrode, intra-, and inter-grain impacts. $Z^*(\omega) = Z' + jZ''$ represents the complex impedance spectroscopy, and Z' and Z'' represent the real and imaginary parts of the complex impedance, respectively. [18,19].

To analyse electrical properties PSM-1735,4NL-LCR,UK.The electrical measurement was in the wide range of frequencies from 100 Hz to 5 MHz and temperature in the range of 25–500°C. The real part of the complex impedance (Z') varying with frequency at different temperatures in the interval of 5^0C in the range of 25^0 to 500^0C is shown in the fig.4. These behaviors are termed as Negative temperature Coefficient of Resistance (NTCR) in both the materials. The release of space charges at grain boundaries gives a decreasing and merge curves at high frequencies for all the temperatures.

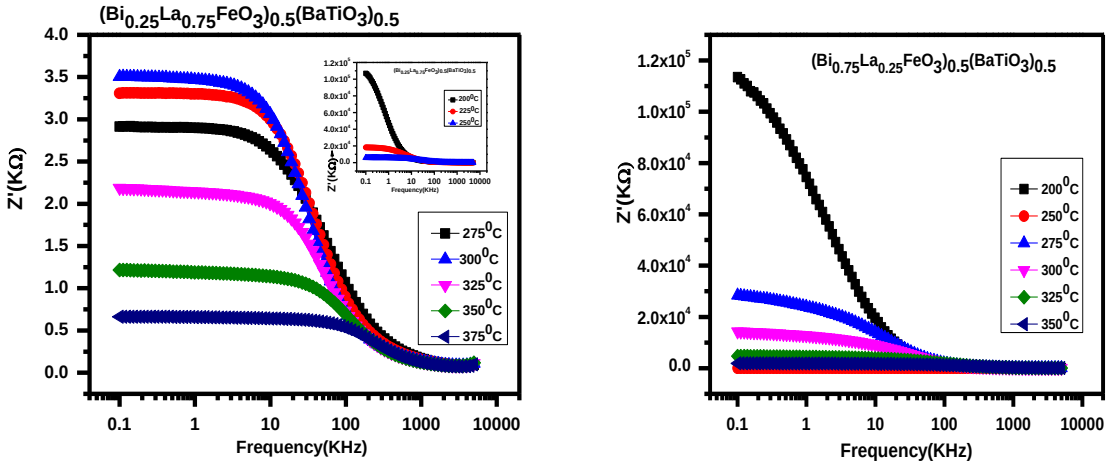

Fig.4 shows variation of Z' with frequency for samples I and 2

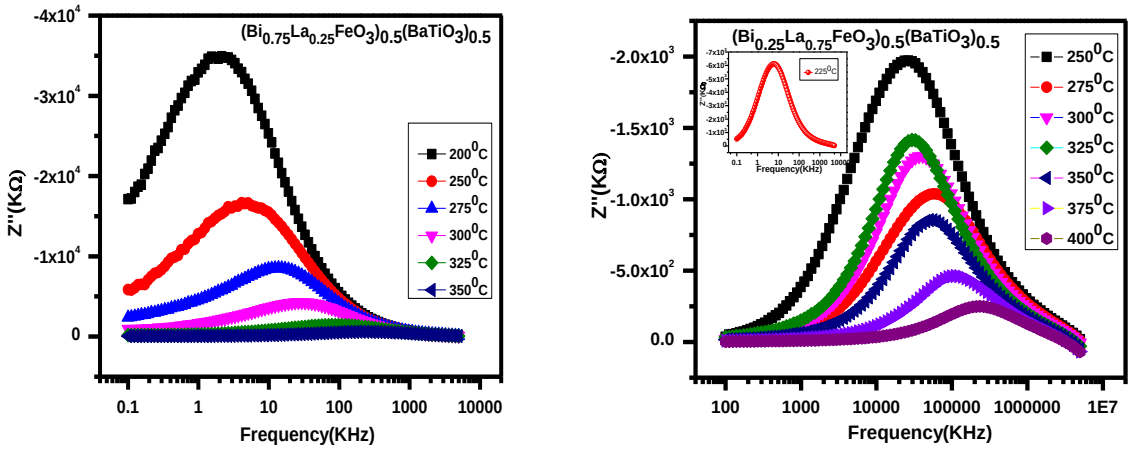

Fig.5 shows variation of z'' with frequency of samples

The relaxed responses of the materials determined by the shift of the imaginary component of impedance (Z") with a specified range of temperatures and frequency. Grain boundaries add to the ridges in the lower part of the frequency, while grain is liable for the flattened part of the higher frequency. Consequently, the reduced temperature relaxation in these specimens originates from stagnant charges, unexplained imperfections and vacancies in oxygen leading to in elevated temperature relaxation. [10–12].

3.5 Leakage Property studies:

The Fig.6 indicates the Current(I) and Voltage (V) variation in the range of 25^0C to 325^0C. Current (I) - Voltage(V) characteristic gives us the information regarding the leakage current and types of charge carriers The leakage feature investigated through I-V characteristic technique suggesting

$(Bi_{0.75}La_{0.25}FeO_3)_{0.5}(BaTiO_3)_{0.5}$ $(Bi_{0.25}La_{0.75}FeO_3)_{0.5}(BaTiO_3)_{0.5}$

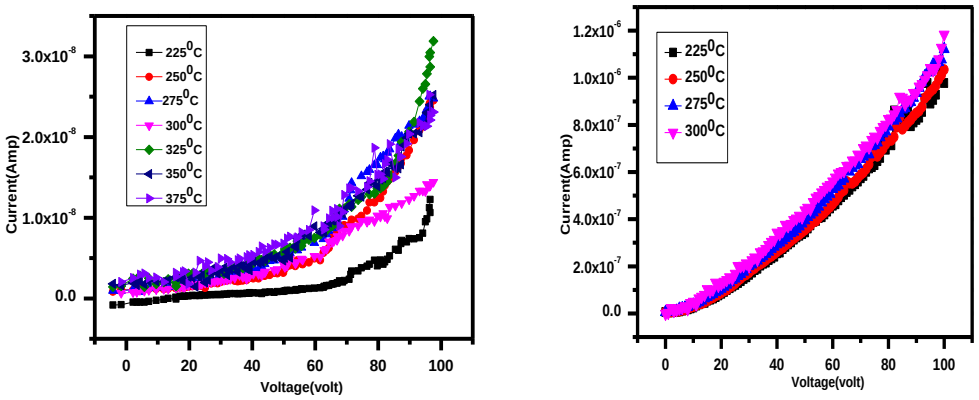

Fig.6: Shows variation of current with voltage of samples

good insulating property of the materials for device oriented application. The leakage current is increasing with the The obtained low leakage-current of the material may be applicable for high temperature applications. To understand the leakage-current properties, we have to consider various types of conduction phenomena like (i) interface-limited conduction phenomena and (ii) bulk-limited conduction phenomena. Schottky mechanism give origination of the interface-limited phenomena from the diference in Fermi levels between a metal and an insulator or semiconductor. The energy diference produces a potential barrier between the metal and the insulator, charges must overcome it. [23] But it was observed that with respect to increase in temperature the leakage current goes in decreasing. Besides it, non-linearity behaviour observed in the leakage current curve with temperature suggests the n-type semi-conducting feature of the materials. With the doping ratio the range of variation changes but the pattern remain same.

4. Conclusion:

La doped BFO-BTOs successfully synthesized in the solid oxide root method which were confirm through XRD diffraction characterizations. The materials formed in the single phase, having orthorhombic and tetragonal crystal structure. The material possess good dielectric property as well as low tangent loss. The NTCR behavior was confirmed through impedance analysis. The I-V curves confirmed the low leakage properties of the materials with doping enhancement and also it gives us the information regarding charge carriers. These materials are free of lead. So, the devices which will be fabricated with the synthesized materials is good for sustainable environment and the doping enhances the suitability of the materials. The obtained low leakage-current may be applicable for high temperature application devices.

5. Declaration of Competing Interest:

The authors declare that they have no known competing financial interests or personal relationships that could have appeared to influence the work reported in this paper.

References:

1. K. Chen, M. Liu, Y. Liu, C. Wang, T. Yoshimura, W. Gong, Y. Le, Tessarollo, J.M.Wang, Nanomaterials based electrochemical sensors for biomedical applications, Chem. Soc. Rev. 63 (3) (2013) 253, https://doi.org/10.1016/j.cyto.2013.06.045.
2. P. Prosposito, L. Burratti, I. Venditti, Silver nanoparticles as colorimetric sensors for water pollutants, Chemosensors 8 (2) (2020) 26, https://doi.org/10.3390/chemosensors8020026.
3. J. BelBruno, Nanomaterials in sensors, Nanomaterials 3 (4) (2013) 572–573.
4. W. Zhang, G.E. Eperon, H.J. Snaith, Metal halide perovskites for energyapplications, Nat. Energy 1 (2016) 16048.
5. P. Gao, M. Grätzel, M.K. Nazeeruddin, Organohalide lead perovskites forphotovoltaic applications, Energy Environ. Sci. 7 (2014) 2448–2463.
6. J. Varignon, M. Bibes, A. Zunger, Origin of band gaps in 3d perovskite oxides,Nat.Commun. 10 (2019) 1658.
7. J. Zhang, Z. Qin, D. Zeng, C. Xie, Metal-oxide-semiconductor based gas sensors:Screening, preparation, and integration, Phys. Chem. Chem. Phys. 19 (2017)6313–6329.
8. P.R. Das, B.N. Parida, R. Padhee, R.N.P. Choudhary, J. Adv.Ceram. 2 (2013) 112–118.
9. T. Wang, J. Hu, H. Yang, L. Jin, X. Wei, C. C Li, F. Yan, Y. Lin, Dielectric relaxation and Maxwell-Wagner interface polarization in Nb2O5 doped 0.65BiFeO3–0.35BaTiO3 ceramics, J. Appl. Phys. 121 (2017), 084103.
10. Rajiv Ranjan, Rajiv Kumar, Nawnit Kumar, Banarji Behera, R.N.P. Choudhury, J. Alloys Compd. 509 (2011) 6388. [52] R.L. White, Review of recent work on the
11. K. Aliouane, A. Guehria-Laidoudi, A. Simon, et al., Study of new relaxor materials in BaTiO3BaZrO3La2/3TiO3 system, Solid State Sci. 7 (11) (2005) 1324–1332.
12. Y. Wang, L. Li, J. Qi, et al., Ferroelectric characteristics of ytterbium-doped barium zirconium titanate ceramics, Ceram. Int. 28 (6) (2002) 657–661.
13. X. Chou, J. Zhai, H. Jiang, et al., Dielectric properties and relaxor behavior of rare-earth (La, Sm, Eu, Dy, Y) substituted barium zirconium titanate ceramics, J. Appl. Phys. 102 (8) (2007), 084106–6.
14. S.E. Hao, L. Sun, J.X. Huang, Preparation and dielectric properties of Dy, Er-doped BaZr0.2Ti0.8O3 ceramics, Mater. Chem. Phys. 109 (1) (2008) 45–49.
15. Qianwei Zhang, W. Cai, Qingting Li, R.L. Gao, G. Chen, X.L. Deng, Z.H. Wang, X. L. Cao, Chunlin Fu, Enhanced piezoelectric response of (Ba, Ca)(Ti, Zr)O3 ceramics by super large grain size and construction of phhase boundary, J. Alloys Compd. 794 (2019) 542–552.
16. G. Catalan, J.F. Scott, Adv. Mater. 21 (2009) 2463–2485.
17. M. Kenzelmann, A.B. Harris, S. Jonas, C. Broholm, J. Schefer, S.B. Kim, C.L. Zhang, S.W. Cheong, O.P. Vajk, J.W. Lynn, Phys. Rev. Lett. 95 (2005), 087206.
18. B. Mohanty, B.N. Parida, R.K. parida, Structural, Dielectric and magnetic behavior of BST modified rare earth Ortho ferrite LaFeO3, Ceram. Int. 46 (Part B) (2020) 16502–16509.
19. T. Wang, J. Liu, L. Kong, H. Yang, F. Wang, C.C. Li, Evolution of the structure, dielectric and ferroelectric properties of Na0.5Bi0.5TiO3-added BaTiO3–Bi(Mg2/ 3Nb1/3)O3 ceramics, Ceram. Int. 46 (2020) 25392–25398.
20. F. Brahma , Bhagyashree Mohanty , S. Bhattacharjee , R.L. Hota , R.K. Parida , B. N. Parida - Investigation of multifunctional characteristics in SmFeO3-BaTiO3 perovskite system for devices, https://doi.org/10.1016/j.mssp.2021.106071, 1369-8001/© 2021 Published by Elsevier Ltd.

21. F. Brahma, R.L. Hota, R.K. Parida, B.N. Parida, Structural and electrical investigation of 'Bi' doped SmFeO3-BaTiO3perovskite systemhttps://doi.org/10.1016/j.matpr.2021.09.362 Materials Today: Proceedings
22. Shangshang Chen, Yehao Deng, Xun Xiao, Shuang Xu, Peter N. Rudd & Jinsong Huang ,Preventing lead leakage with built-in resin layers for sustainable perovskite solar cells Nature Sustainability **volume 4**, pages636–643 (2021)
23. Rutuparna Das, R. N. P. Choudhary, Structural, electrical, and leakage-current characteristics of double perovskite: Sm2CoMnO6, https://doi.org/10.1007/s00339-019-3163-y, Applied Physics A (2019) 125:864.